Nanoscale

RSC Publishing

PAPER

View Article Online
View Journal | View Issue

Cite this: *Nanoscale*, 2013, **5**, 2114

Giant magnetic moments of B and C doped cuboctahedral Mn_{13} clusters†

Menghao Wu* and Puru Jena

Received 12th November 2012
Accepted 3rd January 2013

DOI: 10.1039/c3nr33612c

www.rsc.org/nanoscale

Using first-principles calculations based on gradient corrected density functional theory we show that an otherwise distorted icosahedric Mn_{13} ferrimagnetic cluster, when doped with six B or C atoms, transforms into a ferromagnetic cuboctahedral cluster with a magnetic moment that is an order of magnitude larger than that of the pure Mn_{13} cluster. The origin of this magnetic transition is attributed to the change in the Mn–Mn interatomic distance resulting from the structural transformation. These doped clusters remain ferromagnetic with giant moments even after the removal of a B or C atom. However, similar doping with N atom does not lead to ferromagnetic ordering and $Mn_{13}N_6$ remains ferrimagnetic with a magnetic moment of only 3 μ_B, just as in its parent Mn_{13} cluster.

Introduction

Study of magnetism continues to be a topic of great current interest because of the role magnets play in various technologies. The realization that the magnetic properties of materials can be further tuned at the nanoscale has spurred considerable interest in nanomaterials where their size, shape, and composition can be used to tailor their magnetic properties. Numerous theoretical and experimental studies over the past three decades have shown that small clusters of some nonmagnetic elements such as V and Rh[1,2] become ferromagnetic while the magnetic moments of clusters of ferromagnetic elements such as Fe[3,6,7] and Co[8] are enhanced over their bulk value. Among the antiferromagnetic elements Mn,[4,5] with its half-filled 3d and filled 4s shell, offers the most interesting magnetic properties. While small Mn clusters containing up to four atoms are ferromagnetic with a high magnetic moment of 5 μ_B per atom,[9–11] Mn clusters with larger sizes become ferrimagnetic with much smaller magnetic moments. For example, Mn_{13} clusters carry a magnetic moment of only 3 μ_B.[12,13]

Making larger Mn clusters ferromagnetic with giant magnetic moment has eluded researchers for a long time. This is particularly important since Mn prefers to carry a magnetic moment of 5 μ_B per atom and thus, a cluster containing n number of Mn atoms can potentially carry a magnetic moment of $5n$ μ_B, provided the coupling is ferromagnetic. Nearly a decade ago Rao and Jena predicted theoretically that Mn clusters up to five atoms can become ferromagnetic when they are capped by a nitrogen atom.[14] Can this trend persist for larger compound Mn clusters? It turned out that an Mn_{13} cluster capped by an N atom has a magnetic moment of only 12 μ_B.[15] To our knowledge, the only related work showing large magnetic moment is that of a *negatively* charged Mn–Au core shell cluster ($Mn_{13}@Au_{20}$), which has a ferrimagnetic ground state with a magnetic moment of 44 μ_B and a low spin state (2 μ_B) is only 0.07 eV higher in energy.[16] No *neutral* clusters containing more than 5 Mn atoms have yet been shown to be ferromagnetic carrying giant magnetic moments. If this is possible, one can envision that clusters mimicking the properties of ferromagnetic rare-earth elements can be synthesized without using a single rare-earth element, a topic of great current interest due to the paucity of rare earths and their strategic importance.

To explore this possibility we focus on the magnetism of the parent Mn_{13} cluster. As mentioned earlier, previous studies have shown that the ground state of the Mn_{13} cluster is a distorted icosahedron (Ih)[12,13] with a small total magnetic moment of 3 μ_B. Seven of the Mn atoms in this cluster have their spins aligned in the same direction while the spins of the other six atoms are aligned in the opposite direction. However, if an Mn_{13} cluster can assume a cuboctahedral structure (Oh), one calculation predicted that it may have a high magnetic moment of 47 μ_B.[17] Unfortunately, this configuration is not preferred as its energy is almost 3 eV higher than that of the distorted icosahedral structure. In fact, Oh structures are much higher in energy than the ground state structures for all the 3d, 4d, and 5d metal clusters studied.[17] We wondered if doping with suitable atoms can stabilize the cuboctahedric phase of Mn_{13} without affecting its magnetic properties and hence lead to a giant magnetic moment. In this work, we demonstrate *via* first-principles calculations that this is indeed possible: the transformation to the cuboctahedral ground state structure of an Mn_{13} cluster can be induced and stabilized by doping it with B or C and high magnetic moments that are an order of

Physics Department, Virginia Commonwealth University, Richmond, VA 23284-2000, USA. E-mail: mwu2@vcu.edu

† Electronic supplementary information (ESI) available: Different isomers of higher energies for $Mn_{13}B_6$, $Mn_{13}C_6$, $Mn_{13}B_5$, and $Mn_{13}C_5$ are collected. See DOI: 10.1039/c3nr33612c

magnitude larger than that of the distorted icosahedral Mn_{13} can be obtained, as a result. In contrast to the $Mn_{13}@Au_{20}$ anion, replacing twenty gold atoms by only five or six B or C atoms it is not only possible to achieve a ferromagnetic *neutral* cluster with a giant magnetic moment, but the high spin state is much more stable than that in the $Mn_{13}@Au_{20}$ *anion*.

Computational methods

The equilibrium structures and the corresponding total energies and magnetic properties of various isomers of B, C, and N doped Mn_{13} clusters were calculated using density-functional-theory (DFT) and the DMol^3 4.1 package.[18,19] The generalized gradient approximation (GGA) for the exchange–correlation potential prescribed by Perdew–Burke–Ernzerhof (PBE)[20] and an all-electron double numerical basis set (DNP) with polarization functions were used to carry out spin-unrestricted DFT calculations. The real-space global cutoff radius is set to be 4.7 Å. After optimization, the forces on all atoms are less than 0.0002 Ha Å^{-1}. To verify the accuracy of our DMol^3 results calculations were repeated using the pseudopotential plane-wave method implemented in the Vienna *ab initio* Simulation Package (VASP).[21,22] The projector augmented-wave pseudopotentials[23,24] and the PBE exchange–correlation functional are used to calculate the energies as a function of total magnetic moment.

Results and discussion

As shown in Fig. 1a, the cuboctahedral (Oh) structure of the pure Mn_{13} cluster has six square facets, which makes it less compact compared to the icosahedric (Ih) structure. We found this structure to be unstable and spontaneously transformed into the distorted Ih structure during optimization. Since every center of the six square faces has considerable empty space, we hypothesized that the cuboctahedral structure may be stabilized by doping a small atom at each of these spaces. In Fig. 1b–d, we respectively placed six B, C, or N atoms at the centers of those squares and re-optimized the corresponding geometries. We denote these structures as $Mn_{13}B_6$, $Mn_{13}C_6$, and $Mn_{13}N_6$. The ground states of $Mn_{13}B_6$ and $Mn_{13}C_6$ are found to be ferromagnetic with magnetic moments of 45 and 41 μ_B, respectively and the structures have perfect Oh symmetry. However, the structure of $Mn_{13}N_6$ is distorted and it is ferrimagnetic with a tiny magnetic moment of 3 μ_B. In Fig. 2a–c we compare the spin density distribution of the ground-state structures of Mn_{13}, $Mn_{13}C_6$ and $Mn_{13}N_6$. Note that in Mn_{13} the coupling is ferrimagnetic with the spins of seven Mn atoms aligned antiparallel to the spins of the other six atoms and in agreement with previous calculations the total magnetic moment of Mn_{13} is 3 μ_B. In $Mn_{13}C_6$ clusters, on the other hand, all the Mn atoms have their spins aligned in the same direction. The C sites are not magnetic and the central Mn atom carries a magnetic moment of 2.82 μ_B while the average magnetic moment of the surface Mn atoms is 3.21 μ_B (see Table 1).

To ensure that the ferromagnetic state is the ground state, we calculated the total energies of $Mn_{13}B_6$ and $Mn_{13}C_6$ clusters for different spin states by using the VASP code. The results are plotted in Fig. 2. The ground state magnetic moments of $Mn_{13}B_6$ and $Mn_{13}C_6$ are 47 and 41 μ_B, respectively. For $Mn_{13}B_6$ the spin state corresponding to the magnetic moment of 47 μ_B is only 0.13 eV lower than the state with a magnetic moment of 45 μ_B. Thus, the results obtained using both DMol^3 and VASP codes are consistent. From Fig. 2 we also find that the low spin states in $Mn_{13}C_6$ are all much higher (more than 0.5 eV) in energy than the ground states, suggesting that the high spin states are stable.

For all the three structures, the doped B, C and N atoms are all slightly above the center of the square faces. Vibrational analysis led to no imaginary frequencies. The lowest vibrational frequency of $Mn_{13}B_6$ is 69.5 cm^{-1} while that of $Mn_{13}C_6$ is 118.3 cm^{-1}. This implies that $Mn_{13}C_6$ is more stable than $Mn_{13}B_6$. This is also consistent with their computed binding energies measured with respect to their dissociation into Mn_{13}, B_6, or C_6 cluster. These values are 12.3 eV for $Mn_{13}B_6$ and 13.0 eV for $Mn_{13}C_6$. We also checked some other isomers of $Mn_{13}B_6$ and $Mn_{13}C_6$, which are based on Ih structures doped by B or C at various locations, as shown in the ESI, Fig. S1†. They are all much higher in energy than the Oh structures in Fig. 1b and c, respectively, suggesting that the Oh structures are the most

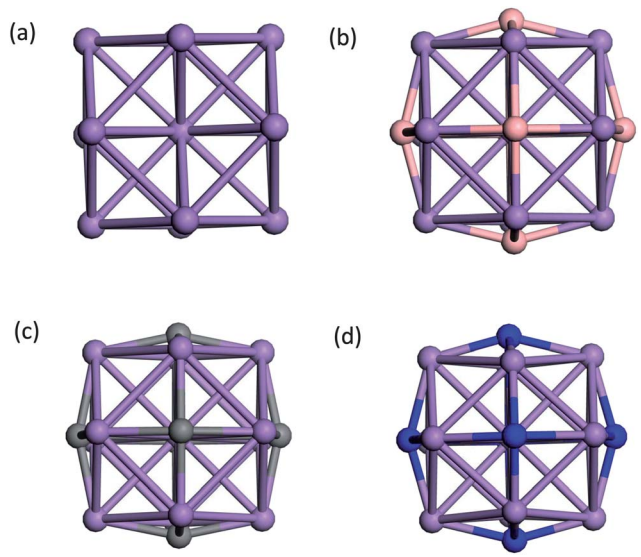

Fig. 1 Geometrical structures of cuboctahedral clusters: (a) Mn_{13}, (b) $Mn_{13}B_6$, (c) $Mn_{13}C_6$, and (d) $Mn_{13}N_6$. Purple, pink, grey, and blue spheres denote Mn, B, C and N atoms, respectively.

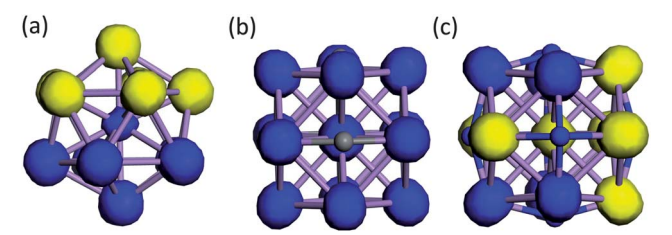

Fig. 2 Spin density distribution of the ground-state: (a) Mn_{13}, (b) $Mn_{13}C_6$ and (c) $Mn_{13}N_6$. Green and red denote spin-up and spin-down densities, respectively, and iso-values of spin density range from −05 to 0.5.

Table 1 The HOMO–LUMO gap Δ, HOMO–LUMO gap in spin-up channel Δ_1 and in spin-down channel Δ_2, the average charge on the surface Mn (Q_s), the central Mn (Q_c), and the doped atom (Q_d), the average Mn–Mn bond length of surface (dss) and surface-core (dsc) atoms, the total magnetic moment (M), and the average absolute value of local magnetic moment of Mn on surface (M_s) and core (M_c) in the ground state of Mn_{13}, $Mn_{13}B_6$, $Mn_{13}C_6$, $Mn_{13}N_6$, $Mn_{13}B_5$ and $Mn_{13}C_5$ clusters

	Δ (eV)	Δ_1 (eV)	Δ_2 (eV)	Q_s (e)	Q_c (e)	Q_d (e)	dss (Å)	dsc (Å)	M (μ_B)	M_s (μ_B)	M_c (μ_B)
Mn_{13}	0.17	0.63	0.17	0.01	−0.12		2.62	2.51	3	3.72	1.30
$Mn_{13}B_6$	0.14	0.41	0.67	0.11	0.10	−0.23	2.77	2.77	45	3.50	3.32
$Mn_{13}C_6$	0.39	0.96	0.39	0.115	0.068	−0.24	2.67	2.67	41	3.21	2.82
$Mn_{13}N_6$	0.25	0.53	0.41	0.13	0.01	−0.26	2.59	2.62	3	3.67	2.15
$Mn_{13}B_5$	0.23	0.23	0.49	0.09	0.07	−0.23	2.76	2.75	48	3.72	3.43
$Mn_{13}C_5$	0.21	0.68	0.21	0.09	0.04	−0.23	2.68	2.67	45	3.59	2.85

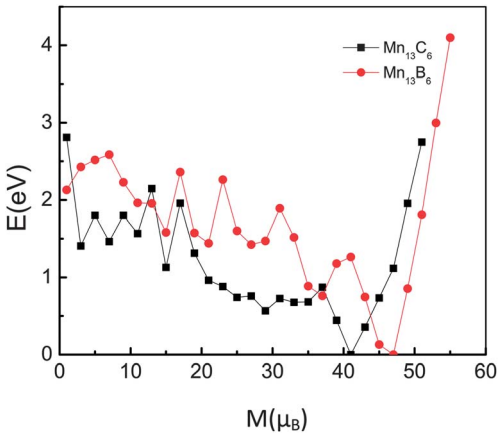

Fig. 3 Relative energies of $Mn_{13}B_6$ and $Mn_{13}C_6$ in different spin states measured with respect to the lowest-energy states.

stable among them. The formation of preferred cuboctahedral structures can be further understood by studying the isomers of Mn_5B and Mn_5C in Fig. 4a–d. Note that the square pyramid Mn_5 with B or C at the square face cap can be regarded as a fragment of the cuboctahedral $Mn_{13}B_6$ or $Mn_{13}C_6$, while the triangular bipyramid structure of Mn_5 with one of the triangular faces capped by B or C atom can be deemed as a part of the Ih $Mn_{13}X_6$ (X = B, C) clusters. It turns out that the energies of the former isomers are 0.04 eV and 0.87 eV lower than that of the latter ones for Mn_5B or Mn_5C, respectively. This trend is in agreement with the ground state structure of $Mn_{13}B_6$ and $Mn_{13}C_6$.

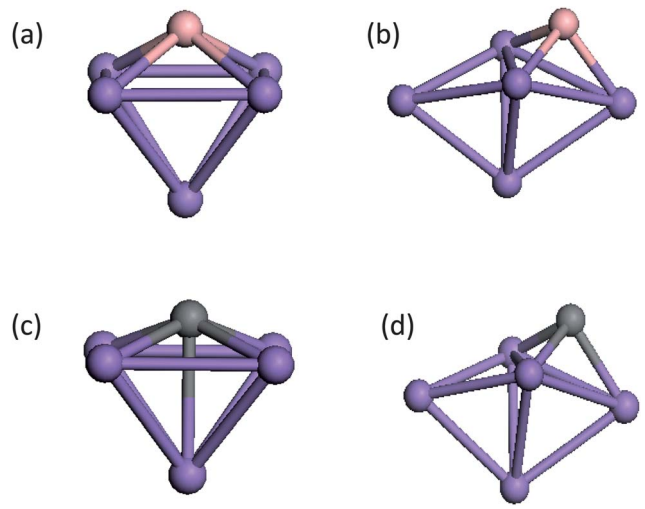

Fig. 4 Geometrical structures of different isomers for Mn_5B (a and b) and Mn_5C (c and d).

In Table 1 we list the HOMO–LUMO gap, the average charge on Mn in pure and doped clusters computed by the Hirshfeld method, the average Mn–Mn bond length, the total magnetic moment, and the average absolute value of local magnetic moment of Mn in the ground state of Mn_{13}, $Mn_{13}B_6$, $Mn_{13}C_6$, and $Mn_{13}N_6$ clusters. $Mn_{13}C_6$ is found to have the largest HOMO–LUMO gap of 0.39 eV. The surface Mn atoms of $Mn_{13}B_6$, $Mn_{13}C_6$, and $Mn_{13}N_6$ clusters carry about the same amount of positive charge (~0.1e) which is transferred to the dopants, and dopants B, C and N all carry around −0.26e per atom. However, there is significant difference in the charges on the central Mn; it is the largest for $Mn_{13}B_6$ and gradually decreases in $Mn_{13}C_6$ and $Mn_{13}N_6$. In pure Mn_{13} the surface atoms carry a negligible charge of +0.01e which is balanced by a −0.12e charge on the central Mn atom. The larger HOMO–LUMO gap and charge transfer in the $Mn_{13}C_6$ cluster compared to that in $Mn_{13}B_6$ and $Mn_{13}N_6$ clusters are consistent with the greater stability of the $Mn_{13}C_6$ cluster.

To understand the origin of the different magnetic behavior of Mn_{13} and $Mn_{13}X$ (X = B, C, and N) clusters we examine the interatomic distances in these clusters in Table 1. A previous report has shown that the exchange coupling of an Mn_2 dimer turns from antiferromagnetic to ferromagnetic as the dimer distance increases.[25] Note also that in ref. 16, the Mn–Mn bond length in $(Mn_{13}@Au_{20})^-$ with a magnetic moment of 44 μ_B is by ~9% larger than that in the bare Mn_{13}^- with a moment of only 2 μ_B. Here the Mn–Mn bond lengths $d(Mn_{13}B_6) > d(Mn_{13}C_6) > d(Mn_{13}N_6) \sim d(Mn_{13})$, which explains why $Mn_{13}N_6$ has a small magnetic moment, and $Mn_{13}B_6$ and $Mn_{13}C_6$ are ferromagnetic with $Mn_{13}B_6$ having the largest magnetic moment. In these clusters the smallest bond length of B–Mn = 2.02 Å > C–Mn = 1.93 Å > N–Mn = 1.87 Å, so it seems that the B and C atoms placed over the center of the Mn squares can effectively increase the distances between the nearest Mn atoms on the surface and therefore stabilize the ferromagnetic coupling between them, similar to the mechanism in ref. 16.

In order to study the dependence of the magnetic properties on the number of dopant atoms we have first calculated the equilibrium structures of $Mn_{13}B_5$ and $Mn_{13}C_5$ by removing one of the dopant atoms and re-optimizing the resulting

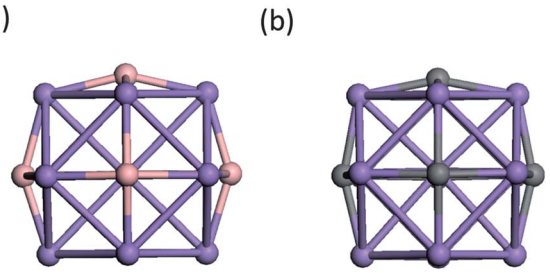

Fig. 5 Geometrical structures of (a) $Mn_{13}B_5$ and (b) $Mn_{13}C_5$.

geometries. The corresponding structures are shown in Fig. 5a and b. The $Mn_{13}B_5$ and $Mn_{13}C_5$ are still ferromagnetic with even larger magnetic moments, namely, 48 and 45 μ_B, respectively (see Table 1). We also studied some other isomers of $Mn_{13}B_5$ and $Mn_{13}C_5$ based on Ih structures doped by B or C at various locations, as shown in Fig. S2.† They are all higher in energy than the structures in Fig. 3a and b, respectively, indicating that doping five carbon or boron atoms is sufficient for stabilizing the cuboctahedral structure and ferromagnetism of Mn clusters. In all the doped clusters in Table 1 we note that the average distance between the Mn atoms on the surface to that in the center or the average distance between surface Mn atoms, with the exception of $Mn_{13}N_6$, is larger than 2.62 Å and these clusters are ferromagnetic. In the Mn_{13} icosahedron the distance between the surface and central atoms is 2.51 Å and the coupling is antiferromagetic. In the $Mn_{13}N_6$ cluster the atoms coupled antiferromagnetically are at a distance of 2.5 Å while those coupled ferromagnetically are at a distance larger than 2.6 Å. Consequently, $Mn_{13}N_6$ has the same magnetic moment as Mn_{13}, namely 3 μ_B.

In summary, we have studied the stability of the cuboctahedral structure of Mn_{13} clusters by doping it with five or six B, C or N atoms. $Mn_{13}B_6$ and $Mn_{13}C_6$ cuboctahedral clusters were not only found to be stable, but they are ferromagnetic with giant magnetic moments, namely 47 and 41 μ_B. The change from ferrimagnetism of Mn_{13} clusters to ferromagnetism in B and C doped Mn_{13} clusters is due to the larger Mn–Mn interatomic distance in the latter. In addition, $Mn_{13}B_5$ and $Mn_{13}C_5$ also turn out to be stable and ferromagnetic with even higher magnetic moments of 48 and 45 μ_B, respectively. These values are an order of magnitude larger than the magnetic moment of the pure Mn_{13} cluster. This study shows that highly magnetic nanoparticles consisting of Mn atoms can be synthesized by suitable doping of non-transition metal elements. This provides a road map for the design and synthesis of magnetic particles that may resemble the properties of rare earth based magnets, but containing little or no rare earth elements. In addition, the surface doped atoms may act as ligands that are commonly present during chemical synthesis to protect the pure metal clusters, rendering them to be used as molecular magnets in spintronics applications such as high performance spin-filters.[26,27]

Acknowledgements

This work was supported in part by a grant from the Department of Energy and used resources of the National Energy Research Scientific Computing Center, which is supported by the Office of Science of the U.S. Department of Energy under contract no. DE-AC02-05CH11231.

Notes and references

1 A. J. Cox, J. G. Louderback and L. A. Bloomfield, *Phys. Rev. Lett.*, 1993, **71**, 923.
2 A. J. Cox, J. G. Louderback, S. E. Apsel and L. A. Bloomfield, *Phys. Rev. B: Condens. Matter Mater. Phys.*, 1994, **49**, 12295.
3 M. Wu, A. K. Kandalam, G. L. Gutsev and P. Jena, *Phys. Rev. B: Condens. Matter Mater. Phys.*, 2012, **86**, 174410.
4 M. B. Knickelbein, *Phys. Rev. Lett.*, 2001, **86**, 5255.
5 M. B. Knickelbein, *Phys. Rev. B: Condens. Matter Mater. Phys.*, 2004, **70**, 014424.
6 I. M. L. Billas, J. A. Becker, A. Châtelain and W. A. de Heer, *Phys. Rev. Lett.*, 1993, **71**, 4067.
7 D. M. Cox, D. J. Trevor, R. L. Whetten, E. A. Rohlfing and A. Kaldor, *Phys. Rev. B: Condens. Matter Mater. Phys.*, 1985, **32**, 7290.
8 X. Xu, S. Yin, R. Moro and W. A. de Heer, *Phys. Rev. Lett.*, 2005, **95**, 237209.
9 S. K. Nayak, B. K. Rao and P. Jena, *J. Phys.: Condens. Matter*, 1998, **10**, 10863.
10 S. K. Nayak and P. Jena, *Chem. Phys. Lett.*, 1998, **289**, 473.
11 P. Bobadova-Parvanova, K. A. Jackson, S. Srinivas and M. Horoi, *J. Chem. Phys.*, 2005, **122**, 014310.
12 M. Kabir, A. Mookerjee and D. G. Kanhere, *Phys. Rev. B: Condens. Matter Mater. Phys.*, 2006, **73**, 224439.
13 T. M. Briere, M. H. F. Sluiter, V. Kumar and Y. Kawazoe, *Phys. Rev. B: Condens. Matter Mater. Phys.*, 2002, **66**, 064412.
14 B. K. Rao and P. Jena, *Phys. Rev. Lett.*, 2002, **89**, 185504.
15 S. Datta, M. Kabir, A. Mookerjee and T. S. Dasgupta, *Phys. Rev. B: Condens. Matter Mater. Phys.*, 2011, **89**, 075425.
16 J. Wang, J. Bai, J. Jellinek and X. C. Zeng, *J. Am. Chem. Soc.*, 2007, **129**, 4110.
17 M. J. Piotrowski, P. Piquini and J. L. F. Da Silva, *Phys. Rev. B: Condens. Matter Mater. Phys.*, 2010, **81**, 155446.
18 B. Delley, *J. Chem. Phys.*, 1990, **92**, 508.
19 B. Delley, *J. Chem. Phys.*, 2000, **113**, 7756.
20 J. P. Perdew, K. Burke and M. Ernzerhof, *Phys. Rev. Lett.*, 1996, **77**, 3865.
21 G. Kresse and J. Hafner, *Phys. Rev. B: Condens. Matter Mater. Phys.*, 1993, **47**, 558.
22 G. Kresse and J. Furthmuller, *Phys. Rev. B: Condens. Matter Mater. Phys.*, 1996, **54**, 11169.
23 P. E. Blöchl, *Phys. Rev. B: Condens. Matter Mater. Phys.*, 1994, **50**, 17953.
24 G. Kresse and D. Joubert, *Phys. Rev. B: Condens. Matter Mater. Phys.*, 1999, **59**, 1758.
25 J. Mejia-Lopez, A. H. Romero, M. E. Garcia and J. L. Moran-Lopez, *Phys. Rev. B: Condens. Matter Mater. Phys.*, 2008, **78**, 134405.
26 S. Barraza-Lopez, K. Park, V. Garcia-Suarez and J. Ferrer, *Phys. Rev. Lett.*, 2009, **102**, 206801.
27 M. Zhou, Y. Q. Cai, M. G. Zeng, C. Zhang and Y. P. Feng, *Appl. Phys. Lett.*, 2011, **98**, 143103.